

# EFFICIENT NON-TOMOGRAPHIC TOOLS FOR THE CHARACTERIZATION OF MULTIPARTITE ENTANGLEMENT

Witłef Wiczeorek<sup>1,2</sup>, Nikolai Kiesel<sup>1,2</sup>, Christian Schmid<sup>1,2</sup> and Harald Weinfurter<sup>1,2</sup>

<sup>1</sup>Max-Planck-Institute of Quantum Optics, D-85748 Garching, Germany

<sup>2</sup>Department for Physics, Ludwig-Maximilians-Universität München, D-80799 München, Germany

The efficient characterization of multipartite entangled states is possible with analysis tools not requiring a full tomographic state estimation. We describe several methods and apply them to two different, genuinely four-partite entangled states, that were recently observed in the experiment.

## 1. INTRODUCTION

Entanglement is the crucial resource in the field of quantum information processing and consequently a better understanding of its properties is very desirable. While for bipartite entangled qubit states many tools for characterization exist and also the experimental implementation of the tools is feasible, the situation for multipartite entangled states is different: The available tools have to be suited for a much greater diversity of entanglement properties, e.g. to analyze all the different entanglement classes [1]. A full experimental characterization via state tomography is increasingly difficult as the number of necessary measurement settings grows exponentially with the number of particles.

In this contribution we focus on efficient, non-tomographic methods to characterize experimentally observed, multipartite entangled states. First steps towards this goal were demonstrated recently, for instance, for the proof of genuine multipartite entanglement [2] or for the analysis of the persistency of entanglement under loss [3]. Such methods can be further optimized by tailoring them to particular properties of states. We show how three important characteristic quantities, the fidelity, the non-separability and the permutation symmetry, can be evaluated with a significantly lower number of measurement settings than required for a complete tomography. Although the determination of these particular properties provides less information than the reconstruction of the complete density matrix, it allows to judge how well state characteristics are reproduced experimentally. This might be important with respect to an experimental application of states in quantum information. Exemplarily we apply the analysis tools to two genuinely four-qubit entangled states: the Dicke state with two excitations  $|D_4^{(2)}\rangle$  [4] and the cluster state  $|C_4\rangle$  [5, 6]. These states are relevant for particular tasks: The state  $|D_4^{(2)}\rangle$  is a resource for telecloning [7], cluster states find an application in one-way quantum computation [6, 8] and are a subgroup of graph states, which play an important role for quantum error correction.

## 2. EXPERIMENTAL REALIZATION OF THE STATES $|D_4^{(2)}\rangle$ AND $|C_4\rangle$

The states were realized experimentally via spontaneous parametric down conversion (SPDC) and linear optics setups, see Fig. (1). We begin with the experimental setup for

the symmetric four-qubit Dicke state with two excitations

$$|D_4^{(2)}\rangle = \frac{1}{\sqrt{6}}(|HHVV\rangle + |HVHV\rangle + |VHHV\rangle + |HVVH\rangle + |VHVV\rangle + |VVHH\rangle),$$

where, e.g.,  $|HHVV\rangle = |H\rangle_a \otimes |H\rangle_b \otimes |V\rangle_c \otimes |V\rangle_d$ , and where  $|H\rangle$  and  $|V\rangle$  mean linear horizontal ( $H$ ) and vertical ( $V$ ) polarization of photons, respectively, and the subscript denotes the spatial mode. The state is the equally weighted superposition of all six possibilities how to distribute two horizontally and two vertically polarized photons onto four spatial modes. We use as photon source the second order emission of type II collinear SPDC from a BBO ( $\beta$ -Barium Borate, 2 mm thick) crystal, where two horizontally and two vertically polarized photons are created. UV pulses with a central wavelength of 390 nm and a power of 600-700 mW from a frequency-doubled mode-locked Ti:Sapphire laser are used to pump the crystal. The SPDC emission is coupled into a single mode fiber that defines the spatial mode. Then, the photons are distributed equally onto four spatial modes  $a, b, c$  and  $d$  via three polarization independent beam splitters. The state  $|D_4^{(2)}\rangle$  is observed if a photon is registered in each output mode. Details of the experimental setup can be found in [4].

The second state to be characterized is the four-qubit cluster state

$$|C_4\rangle = \frac{1}{2}(|HHHH\rangle + |HHVV\rangle + |VVHH\rangle - |VVVV\rangle).$$

The state  $|C_4\rangle$  was realized experimentally by entangling two polarization entangled photon pairs via a controlled phase gate [9]. The pairs  $(|\phi^+\rangle_{ab'} = 1/\sqrt{2}(|HH\rangle_{ab'} + |VV\rangle_{ab'}))$  in modes  $a$  and  $b'$ , and  $|\phi^+\rangle_{c'd}$  in modes  $c'$  and  $d$  were created by the first order emission of non-collinear type II SPDC in double pass configuration using the same pump laser system as above. The linear optical gate between modes  $b'$  and  $c'$  was implemented experimentally via a second order interference on a polarization dependent beam splitter (PDBS). A phase shift is applied only in the case that both photons carry vertical polarization:  $|VV\rangle_{b'c'} \rightarrow -|VV\rangle_{bc}$ . The state  $|C_4\rangle$  is observed if a photon is registered in each of the four modes. Details can be found in [5, 9].

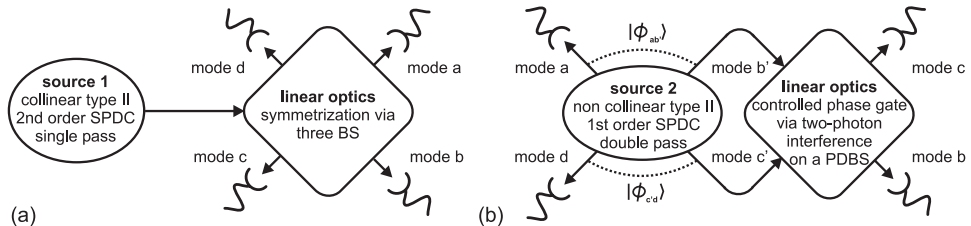


Figure 1: Schematic setups for the observation of the states  $|D_4^{(2)}\rangle$  (a) and  $|C_4\rangle$  (b) in modes  $a, b, c$  and  $d$ . (PD)BS means a polarization independent (dependent) beam splitter.

### 3. QUALITY OF STATE PREPARATION

In the experiment one is interested in the quality of the prepared state, i.e. how close is the experimental to the desired state. For this purpose we take the fidelity [10]

as a measure. The fidelity  $F_\Phi$  of a state  $\rho_{exp}$  with respect to a desired state  $|\Phi\rangle$  is:  $F_\Phi = \langle \Phi | \rho_{exp} | \Phi \rangle = \sum_{i,j,k,l} S_{i,j,k,l} \langle \Phi | \sigma_i \sigma_j \sigma_k \sigma_l | \Phi \rangle$ , where the density matrix  $\rho_{exp}$  was decomposed in tensor products of Pauli spin operators  $\sigma_r$  with  $r \in \{0, x, y, z\}$ . In general, full knowledge of the experimental state requires a measurement of all its correlations  $S_{i,j,k,l}$  in order to determine its density matrix, yet for four qubits these are 256 values. Fortunately, only the correlations that are non-zero, i.e.  $\langle \Phi | \sigma_i \sigma_j \sigma_k \sigma_l | \Phi \rangle \neq 0$ , enter the determination of the fidelity and thus the number of measurement settings is drastically reduced.

The state  $|D_4^{(2)}\rangle$  exhibits only 40 non-zero correlations. These 40 values can be derived from 21 measurement settings in the standard bases  $(H/V)$ ,  $(\pm 45^\circ)$  and  $(L/R)$  corresponding to the eigenvectors of  $\sigma_z$ ,  $\sigma_x$  and  $\sigma_y$ , where  $|\pm 45^\circ\rangle = 1/\sqrt{2}(|H\rangle \pm |V\rangle)$  and  $|L/R\rangle = 1/\sqrt{2}(|H\rangle \pm i|V\rangle)$ . A fidelity of  $F_{D_4^{(2)}} = 0.844 \pm 0.008$  was found [4]. The determination of the fidelity for the cluster state needs even less measurement settings. One can profit from the fact that the cluster state, as a four-qubit graph state, is completely describable by its 16 stabilizers [11]. Therefore, the fidelity of the cluster state equals the averaged expectation value of the stabilizer operators and a measurement of the respective correlations is sufficient to evaluate it. These 16 correlations can be derived from only nine measurement settings and result in  $F_{C_4} = 0.741 \pm 0.013$  [5]. The deviation of the experimental from the ideal states can be attributed to a remaining degree of distinguishability of the four photons, higher order emissions of the SPDC process and imperfections in the optical components.

#### 4. EFFICIENT WITNESS OPERATORS

Another important question is whether the experimental state exhibits genuine multipartite entanglement. Witness operators are an efficient tool to prove this. A generic witness that detects a state  $|\Phi\rangle$  as genuine multi-partite entangled is given by  $\mathcal{W} = \alpha \mathbb{1} - |\Phi\rangle\langle\Phi|$ , where  $\alpha = \max_{|\psi\rangle \in B} |\langle\psi|\Phi\rangle|^2$  and  $B$  denotes the set of biseparable states [2]. This construction guarantees that the expectation value of  $\mathcal{W}$  on all biseparable states is positive, but negative on the genuine multi-partite entangled state  $|\Phi\rangle$ . Effectively the expectation value of  $\mathcal{W}$  can be expressed in terms of the fidelity:  $Tr[\mathcal{W}\rho_{exp}] = \alpha - \langle\Phi|\rho_{exp}|\Phi\rangle$ . Therefore, its determination requires as many measurements as are necessary for the determination of the fidelity. In the following we apply more efficient witnesses [11,12] that are tailored to particular features of the states  $|D_4^{(2)}\rangle$  and  $|C_4\rangle$ , resulting in a reduced number of necessary measurements.

One can construct an efficient entanglement witness  $\mathcal{W}_{D_4^{(2)}}$  for the state  $|D_4^{(2)}\rangle$  from a measurement of the collective spin squared in the  $x$ - and  $y$ -direction ( $J_x^2$  and  $J_y^2$ ) [12]:  $\mathcal{W}_{D_4^{(2)}} = \alpha \mathbb{1} - (J_x^2 + J_y^2)$ , where  $\alpha = 7/2 + \sqrt{3} \approx 5.23$  is the maximal expectation value of  $J_x^2 + J_y^2$  reached by biseparable states and where  $J_{x/y} = 1/2 \sum_k \sigma_{x/y}^k$  with e.g.  $\sigma_x^3 = \mathbb{1} \otimes \mathbb{1} \otimes \sigma_x \otimes \mathbb{1}$ . Thus, only two measurement settings suffice for the experimental determination of  $\mathcal{W}_{D_4^{(2)}}$ . Rewriting  $J_x^2 + J_y^2$  as  $J^2 - J_z^2$ , where  $J = (J_x, J_y, J_z)$ , we get for  $|D_4^{(2)}\rangle$  a total spin squared of  $\langle J^2 \rangle = 6$  due to its permutation symmetry and  $\langle J_z^2 \rangle = 0$ , resulting in an expectation value for the witness of  $\approx -0.77$ . Experimentally, from data

shown in Fig. (2a), we find a value of  $\text{Tr}[\mathcal{W}_{D_4^{(2)}}\rho_{exp}] = -0.35 \pm 0.02$ . For the cluster state it was shown that the witness can be constructed from its stabilizers [11]:  $\mathcal{W}_{C_4} = 3 \cdot \mathbb{1}^{\otimes 4} - \frac{1}{2}(\sigma_z^{(a)}\sigma_z^{(b)} + \mathbb{1})(\sigma_z^{(b)}\sigma_x^{(c)}\sigma_x^{(d)} + \mathbb{1}) - \frac{1}{2}(\sigma_z^{(c)}\sigma_z^{(d)} + \mathbb{1})(\sigma_x^{(a)}\sigma_x^{(b)}\sigma_z^{(c)} + \mathbb{1})$ , where  $\sigma_i^{(j)}$  is the Pauli matrix  $i$  acting on qubit  $j$ . Again only two local measurement settings suffice for its determination. Theoretically a value of  $-1$  is expected, experimentally we find  $\text{Tr}[\mathcal{W}_{C_4}\rho_{exp}] = -0.299 \pm 0.050$ , which is derived from the measurements displayed in Fig. (2b). In both cases, negative expectation values clearly prove that both observed states are genuine four-partite entangled.

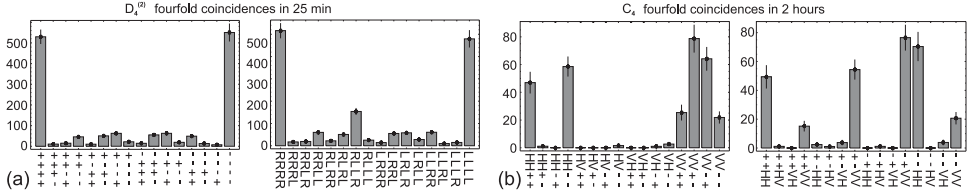


Figure 2: Fourfold coincidence counts of the states  $|D_4^{(2)}\rangle$  (a) and  $|C_4\rangle$  (b) sufficient for the evaluation of their witnesses. For  $|D_4^{(2)}\rangle$  measurements in the  $(\pm 45^\circ)$  and  $(L/R)$  bases of all qubits are displayed. For  $|C_4\rangle$  a measurement in  $(H/V)$  of qubits  $a$  and  $b$  and  $(\pm 45^\circ)$  of qubits  $c$  and  $d$  is shown on the left of (b), on the right the bases are exchanged.

## 5. PERMUTATION SYMMETRY OF THE STATES

Non-tomographic methods not only allow to verify genuine four-partite entanglement, but also to examine further properties. We show that permutation symmetry can be analyzed with few local measurements. It is interesting to observe that, even though permutation symmetry alone is not an entanglement criterion, important multipartite entangled states are symmetric, like for instance the GHZ and the W state as well as the examples we deal with. Here, we analyze how well the symmetries of the desired states are reproduced by the experimentally obtained ones. We will discuss how deviations are connected with the experimental implementation of the states.

Permutation is described by the swap operator  $S_{ba}$  [10] exchanging photons  $a$  and  $b$ :  $S_{ba}|HH\rangle_{ab} = |HH\rangle_{ba}$ ,  $S_{ba}|HV\rangle_{ab} = |HV\rangle_{ba}$ ,  $S_{ba}|VH\rangle_{ab} = |VH\rangle_{ba}$  and  $S_{ba}|VV\rangle_{ab} = |VV\rangle_{ba}$ . The subscript of the ket denotes the spatial mode of the photon and the subscript of the swap operator denotes the new ordering of the photons after its application. For pure states, the expectation value of the swap operator  $\langle S \rangle = \langle \psi | S | \psi \rangle$  has a simple interpretation as the overlap between a pure state  $|\psi\rangle$  and its permuted counterpart  $S|\psi\rangle$ . It takes values between  $-1$  and  $+1$  representing a completely antisymmetric ( $|\psi^-\rangle$ ) and symmetric state (e.g.  $|\psi^+\rangle$ ), respectively [where  $|\psi^\pm\rangle = 1/\sqrt{2}(|HV\rangle \pm |VH\rangle)$ ]. When extending this scheme to mixed states  $\rho$  we find two possible ways of how to look at permutation symmetry. One is, as for pure states, by taking the expectation value of the swap operator  $s = \text{Tr}[S\rho]$ . This value gives the weighted average of the pure state symmetries in the decomposition of the mixed state:  $s = \text{Tr}[S\rho] = \sum_i p_i \langle \psi_i | S | \psi_i \rangle$ , where  $p_i$  is the probability to contain the state  $|\psi_i\rangle$ . However, this is not the overlap

between a mixed state  $\rho$  and its permuted counterpart  $S\rho S$  anymore. The overlap is given by:  $s_\rho = \text{Tr} \left[ \sqrt{\sqrt{\rho} \cdot S\rho S \cdot \sqrt{\rho}} \right]$ . The expectation value  $s$  allows, in contrast to  $s_\rho$ , to detect antisymmetry, as  $s$  captures the individual symmetries of pure states in the decomposition of the mixed state. To illustrate this we consider two-qubit white noise:  $\rho_{noise} = 1/4(|\phi^-\rangle\langle\phi^-| + |\phi^+\rangle\langle\phi^+| + |\psi^+\rangle\langle\psi^+| + |\psi^-\rangle\langle\psi^-|)$ . For  $\rho_{noise}$  we obtain  $s = 1/2$ , but  $s_\rho = 1$ . This difference stems from the fact that  $s$  detects the state  $|\psi^-\rangle$  as antisymmetric, whereas the remaining three states as symmetric. In contrast,  $s_\rho$  evaluates the mixed state as a whole and  $\rho_{noise}$  is symmetric when exchanging particles, thus  $s_\rho$  yields 1. Which of the two types for evaluating the symmetry of mixed states is chosen for an experimental determination depends on the problem to be analyzed. Here, we pursue to study  $s$ , i.e. the expectation value of the swap operator, as for its experimental determination only three local measurements are required: The swap operator can be decomposed into  $S_{ba} = 1/2(\mathbb{1}^{(a)} \otimes \mathbb{1}^{(b)} + \sigma_z^{(a)} \otimes \sigma_z^{(b)} + \sigma_x^{(a)} \otimes \sigma_x^{(b)} + \sigma_y^{(a)} \otimes \sigma_y^{(b)})$ . In contrast, the experimental determination of  $s_\rho$  requires a full tomographic state estimation.

For four qubits we find 24 possible permutations. These form a group and can be obtained by concatenation of swap operators between different pairs of qubits. To obtain all 24 permutations one only needs to consider three generators from the group: we choose the swap operators acting on neighboring qubits:  $S_{bacd}$ ,  $S_{acbd}$  and  $S_{abdc}$ . The state  $|D_4^{(2)}\rangle$  is completely symmetric with respect to all 24 permutations and therefore the expectation value of the swap operators with  $|D_4^{(2)}\rangle$  is +1. To test how well the symmetry is reproduced by the experimental state we determined the expectation values for the chosen swap operators depicted in Table (1). The values are close to +1 and thus reflect the high symmetry of the experimental state. Small deviations between the values are observed. As imperfections in the photon source can only lower all values by the same amount, the differences between the values can solely be attributed to imperfections in the linear optics setup. The permutation symmetry of the cluster state  $|C_4\rangle$  is different. It is only symmetric with respect to exchange of particles  $a$  and  $b$  ( $S_{bacd}$ ) and  $c$  and  $d$  ( $S_{abdc}$ ), while not being fully symmetric for exchange of  $b$  and  $c$  ( $S_{acbd}$ ). The expectation value of  $S_{acbd}$  is +0.5 in theory. Table (1) shows the experimentally obtained values. The SPDC emission provides the bipartite state  $|\phi_{ab}\rangle|\phi_{cd}\rangle$  that already possesses the permutation symmetry of the desired state  $|C_4\rangle$ . The observed high values for  $S_{bacd}$  and  $S_{abdc}$  support the fact that the source emits a very symmetric state that is also not disturbed by the phase gate. However, the value of  $S_{acbd}$  is higher than the theoretical one. We attribute this to the non-perfect indistinguishability of the photons at the PDBS causing a non-perfect two photon interference, in agreement with the interpretation in [5, 9]. That results in a higher probability to observe the symmetric term  $|VVVV\rangle$  and thus makes the resulting mixed state more symmetric with respect to  $S_{acbd}$ .

$\langle S_{bacd} \rangle$		$0.92 \pm 0.02$		$0.98 \pm 0.07$
$\langle S_{acbd} \rangle$	$ D_4^{(2)}\rangle$	$0.97 \pm 0.02$	$ C_4\rangle$	$0.62 \pm 0.09$
$\langle S_{abdc} \rangle$		$0.94 \pm 0.02$		$0.98 \pm 0.08$

Table 1: Expectation values for three swap operators applied to  $|D_4^{(2)}\rangle$  and  $|C_4\rangle$ .

## 6. SUMMARY

In conclusion, we have described efficient, non-tomographic methods for state characterization and applied them to two genuinely four-partite entangled states experimentally: the Dicke state with two excitations and the cluster state. While evaluation of the state's fidelity requires 21 and 9 measurement settings, respectively, a proof of genuine four-partite entanglement requires only two measurement settings. Together with the efficient evaluation of permutation symmetry these methods represent useful tools for the analysis of experimentally observed multipartite quantum states.

## ACKNOWLEDGMENTS

We acknowledge the support of this work by Deutsche Forschungsgemeinschaft through the DFG-Cluster of Excellence "Munich-Centre for Advanced Photonics" and the European Commission through the EU Project QAP. We are very thankful for a fruitful collaboration with Otfried Gühne, Enrique Solano, Géza Tóth, Rupert Ursin and Ulrich Weber. One of the authors, W. W., acknowledges support by QCCC of the Elite Network of Bavaria and the Studienstiftung des deutschen Volkes.

## REFERENCES

- [1] W. Dür *et al.*, Phys. Rev. A **62**, 062314 (2000); F. Verstraete *et al.*, Phys. Rev. A **65**, 052112 (2002).
- [2] D. Bruss *et al.*, J. Mod. Opt. **49**, 1399 (2002); M. Bourennane *et al.*, Phys. Rev. Lett. **92**, 087902 (2004).
- [3] M. Bourennane *et al.*, Phys. Rev. Lett. **96**, 100502 (2006).
- [4] N. Kiesel *et al.*, Phys. Rev. Lett. **98**, 63604 (2007).
- [5] N. Kiesel *et al.*, Phys. Rev. Lett. **95**, 210502 (2005).
- [6] P. Walther *et al.*, Nature **434**, 169 (2005).
- [7] M. Muraio *et al.*, Phys. Rev. A **59**, 156 (1999).
- [8] R. Raussendorf and H. J. Briegel, Phys. Rev. Lett. **86**, 5188 (2001).
- [9] N. Kiesel *et al.*, Phys. Rev. Lett. **95**, 210505 (2005).
- [10] M. A. Nielsen and I. L. Chuang, *Quantum Computation and Quantum Information* (Cambridge University Press, 2000).
- [11] G. Tóth and O. Gühne, Phys. Rev. Lett. **94**, 060501 (2005); G. Tóth and O. Gühne, Phys. Rev. A **72**, 022340 (2005);
- [12] G. Tóth, J. Opt. Soc. Am. B **24**, 275-282 (2007).